

Disorder-quenched Kondo effect in mesoscopic electronic systems

Stefan Kettemann^{1,2} and Eduardo R. Mucciolo³

¹ Institut für Theoretische Physik, Universität Hamburg, Jungiusstraße 9, 20355 Hamburg, Germany,

² Max-Planck Institute for Physics of Complex Systems, Nöthnitzer Straße 38, Dresden, Germany, and

³ Department of Physics, University of Central Florida, P.O. Box 162385, Orlando, FL 32816-2385, USA

(Dated: January 25, 2020)

The screening of magnetic moments in metals, the Kondo effect, is found to be quenched with a finite probability in the presence of nonmagnetic disorder. It is shown analytically that the distribution of the Kondo temperature has a finite width due to wave function correlations within an energy interval of order $1 = \tau$, where τ is the elastic scattering time. This width remains finite in the limit of vanishing level spacing Δ . When time-reversal symmetry is broken either by applying a magnetic field or by increasing the concentration of magnetic impurities, the distribution of Kondo temperatures becomes narrower. The probability that a magnetic moment remains free down to zero temperature is found to increase with disorder strength. Experimental consequences for disordered metals are studied. In particular, it is shown that the presence of magnetic impurities with a small Kondo temperature enhances the electron's dephasing rate at low temperatures in comparison to the clean metal case.

PACS numbers: 72.10.Fk, 72.15.-m, 75.20.Hr

Keywords: Kondo effect, Anderson localization, phase coherence

I. INTRODUCTION

A local magnetic impurity changes the ground state of a Fermi liquid due to the correlations created by the antiferromagnetic exchange interaction between its localized spin and the delocalized electrons.^{1,2} At temperatures below the Kondo temperature T_K the spin of the magnetic impurity is screened by the formation of a singlet state with the conduction electrons.^{3,4} Disorder affects the formation of this Kondo singlet in various ways. In particular, the Kondo temperature may depend on the positioning of the magnetic impurities in the host lattice. Thus, for a sample containing many magnetic impurities, T_K may be distributed due to fluctuations of the microscopic exchange coupling.^{5,6,7} Impurities (magnetic or nonmagnetic) and lattice defects also cause fluctuations in the local density of states (LDOS) of the conduction electrons at the magnetic impurity site. Thus, the distributions of the Kondo temperature and of the LDOS are related in a disordered metal.^{8,9}

In this paper we explore the consequences of nonmagnetic disorder for the Kondo effect. We base our study on the statistical properties of T_K in the different dynamics regimes of a disordered metal. Note that the Kondo temperature accounts for a crossover rather than a sharp transition and that may raise the question whether T_K is sufficiently well defined. In response to that, we also note that by fitting physical quantities such as the spin susceptibility and the electron dephasing rate versus temperature against the corresponding universal scaling function, it is possible in principle to extract T_K and then investigate its sample-to-sample fluctuations. Below we show that these fluctuations may have a significant impact on the properties of the metal even in the thermodynamic, infinite-volume limit.

It is useful to compare the magnitude of T_K to other relevant energy scales of a metallic sample. These scales are the mean level spacing $\Delta = 1 = L^d$, the Thouless energy $E_c = D_e = L^2$, and the elastic scattering rate $1 = \tau$. Here,

denotes the density of states at the Fermi level, $D_e = v_F^2 = d$ is the diffusion constant, and d is the dimensionality of diffusion (we have set $\hbar = k_B = 1$). This comparison allows one to establish several distinct regimes, as sketched in Fig. 1. We note that, in practice, T_K does not exceed $1 = \tau$ in metals, therefore standard perturbation theory in the disorder potential may not be used to describe the effect of disorder on the Kondo effect. However, there is a large regime of experimental interest where a diagrammatic expansion may be used, namely, $E_c < T_K < 1 = \tau$.¹⁰ For small samples, when $\Delta < T_K < E_c$, random matrix theory (RMT) can be applied and the distribution of Kondo temperatures is expected to scale with Δ alone. In the opposite limit, when the grain is so large that the localization length ξ is smaller than the linear size L , the Thouless energy and the global level spacing are irrelevant and the Kondo temperature is determined by the mean level spacing for states localized in the vicinity of the magnetic impurity, $1 = \tau = \Delta^d$.^{11,12,13} In this case, one can expect the distribution of Kondo temperatures to scale with Δ instead of τ . Finally, when T_K is smaller than the spacing between neighboring energy levels at the Fermi surface (either Δ or E_c), the distribution of T_K will be mainly determined by the fluctuations of the wave functions and level spacing of the two eigenstates closest to the Fermi energy. Accordingly, in this regime the Kondo temperature is determined by the coupling of the magnetic impurity to a two-level system (2LS).

The paper is organized in the following way. In Sec. II we introduce the problem of finding the distribution of the Kondo temperature as defined by an integral equation. In Sec. III, for reference, we briefly present the solution of the integral equation in the clean limit using a picket-fence spectrum (equidistant energy levels). In Sec. IV, we consider the RMT regime. We present the analytical results obtained for the distribution of T_K by taking into account only wave function fluctuations. We compare these with numerical results obtained from simulations of random matrix ensembles. It is found that the distribution of T_K deviates from the Gaussian behavior even for $T_K \ll \Delta$, in agreement with an analytical prediction. The ra-

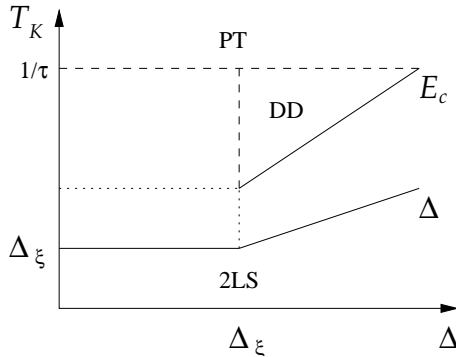


FIG. 1: Overview of the different regimes of a mesoscopic Kondo system of linear size L , as parametrized by the system's mean level spacing $\tau = 1 = L^d$ and the unaveraged Kondo temperature of a single magnetic impurity T_K . E_c is the Thouless energy, $1 =$ is the elastic scattering rate, and $\xi = 1 = L^d$, with ξ being the localization length. The acronyms denote: Two levels coupled to the magnetic impurity (2LS), random matrix theory (RMT), diagrammatic expansion in diffusion ladder diagrams (DD), and perturbative regime, (PT), with $1 = g = E_c$ as the small expansion parameter. We only consider metallic systems where the relation $1 = E_F$ is fulfilled.

tio between the standard deviations of T_K for the orthogonal and unitary ensemble is found numerically to be equal to $\sqrt{2}$ for a wide range of exchange couplings J , in agreement with analytical calculations. Furthermore, it is shown numerically that a finite number of free moments persists to exist in this regime. This result is consistent with an analytical calculation based on the 2LS approximation.

The central results of our paper are presented in Sec. VI. There, the distribution, average, and standard deviation of the Kondo temperature are studied as function of disorder strength by taking eigenstates and eigenenergies from an Anderson's disordered tight-binding model. The average and standard deviation are derived analytically as function of J , E_c , and the disorder parameter g and compared with the numerical results. The analytical and numerical results agree well within their range of validity. The analytical calculations show that the average Kondo temperature is enhanced by weak disorder. Disorder also induces a *finite width* in the distribution of T_K which is shown to persist even in the infinite sample, thermodynamic limit. This effect is due to the existence of local correlations between eigenfunctions at different energies within a macroscopically large energy interval $1 =$. The numerical simulations show that there are disorder configurations where no finite value of T_K exist in the lowest order self-consistent approximation, indicating that in those cases the magnetic moment is not screened by the conduction electrons. The relative number of free moments is studied as a function of the exchange coupling J and disorder strength g . We find that there is a finite probability of having free moments even for values of J such that the average Kondo temperature hT_K is much larger than the mean level spacing τ .

The dependence of the distribution of the Kondo temperature on the concentration of magnetic impurities is studied in Sec. VII. We find a counter-intuitive result at first glance,

namely, that the distribution becomes *narrower* when increasing the concentration. This effect is explained by the reduction of localization effects caused by breaking time-reversal invariance. We also consider whether additional correlations between wave functions induced by breaking of time reversal symmetry⁴⁷ within an interval of order $1 = \xi$ can lead to an enhancement of the width of the distribution of T_K . We find that while the width increases by a factor ξ as compared to the the pure RMT ensembles, it nevertheless vanishes in the thermodynamic limit when $\xi \rightarrow 0$, and therefore is negligible with respect to the broadening caused by wave functions correlations beyond RMT.

In Sec. VIII, we consider the question whether the distribution of Kondo temperatures and the existence of free magnetic moments in disordered metals have any consequences for the temperature dependence of the electron's dephasing rate. We find that nonmagnetic disorder combined with spin scattering due to magnetic impurities increases the dephasing rate at temperatures $T < T_K$. The dephasing rate is readily accessible in transport experiments by measuring weak-localization corrections to the resistance.

Finally, in Sec. IX we summarize our results and make our concluding remarks. An Appendix with the derivation of the integral equation for the Kondo temperature in a one-loop approximation for a disordered sample is included, together with a critical discussion of its validity.

II. FORMULATION OF THE PROBLEM

We will consider a single magnetic impurity in an isolated, phase-coherent metallic grain where the energy levels are well separated, a system previously referred in the literature as the Kondo box.^{14,15} To determine T_K , we will adopt the following self-consistent equation:^{9,16,17}

$$1 = \frac{J}{2N} \sum_{n=1}^N \frac{j_n(0) \tau}{E_n - E_F} \tanh \frac{E_n - E_F}{2T_K} ; \quad (1)$$

where N is the number of states in the spectrum, $\tau = L^d$ is the grain volume, E_F is the Fermi energy, and J is the exchange coupling between the magnetic impurity and the delocalized electrons. The eigenenergies and eigenfunctions of the grain are, respectively, E_n and $j_n(r)$, while the impurity is located at $r = 0$. Equation (1) is obtained from second-order perturbation theory in Appendix A. A similar expression can be obtained from the zero-temperature, self-consistent solution of the one-loop renormalization group (RG) equation.^{4,18} However, in that case one misses the \tanh factor (which accounts for the finite-temperature occupation numbers) and the result is only valid for $T_K \gg \tau$. While the approximations involved in deriving Eq. (1) are not sufficient for describing the properties of the system below T_K , it is important to remark that Eq. (1) does yield a good estimate for the Kondo temperature, which is the relevant scale for the low-temperature behavior of Kondo systems. The two-loop correction has been found to change the Kondo temperature by

a factor $\frac{1}{\sqrt{J=D}}$.⁴ In the thermodynamic limit (infinite volume), the physics at temperatures $T = T_K$ is known to be that of an effective Fermi liquid, where the Kondo temperature determines the Landau parameters.³ For example, the effective mass, the density of states, and thereby the specific heat become enhanced by a factor $1 + n_m = (T_K)$, while the paramagnetic susceptibility is enhanced by a factor $1 + 2n_m = (T_K)$,^{2,3} where n_m is the concentration of magnetic impurities.

It will be convenient to rescale Eq. (1) to a dimensionless form, in which case it becomes

$$1 = \frac{1}{2x} \sum_{n=1}^{N^2} \frac{x_n}{s_n} \tanh \frac{s_n}{2} ; \quad (2)$$

where $x = D = J$, $T_K = D$, $x_n = j_n(x)$ is the probability density of the eigenstate, and $s_n = (E_n - E_F)$ is the eigenenergy measured relative to the Fermi energy in units of J .

In the following, we assume that the Fermi energy is in the middle of two energy levels, so that the number of electrons in the Kondo box is even. (For an odd number of electrons, the unpaired electron at the Fermi energy forms a singlet with the magnetic impurity with binding energy J and the problem becomes trivial.) Using Eq. (2), the distribution of Kondo temperatures is determined by

$$P(T_K) = \frac{d}{dT_K} \left. \frac{Z_{D=J}}{Z_0} \right|_0 dx x F(T_K) ; \quad (3)$$

where

$$F(T_K) = \frac{1}{2} \sum_{n=1}^{N^2} \frac{x_n}{s_n} \tanh \frac{s_n}{2} ;$$

We note that a similar expression appears in the calculation of the distribution of NMR-Knight shifts for metallic grains with a finite level width.^{19,20,21} There, an exact solution of the problem was derived within RMT in the limit $N \rightarrow 1$. However, two aspects make the problem defined by Eq. (3) much harder to solve. First, in the NMR-Knight shift case, instead of Eq. (4), the calculation involves a sum over terms which behave as $1/(s_n^2 + J^2)$, decaying faster than $1/s_n$ at large energies. Second and more importantly, since the Kondo temperature enters in Eq. (4) essentially as the low-energy cut-off of the sum, we cannot apply the techniques used in Refs. 19,20,21 to the calculation of the distribution of Kondo temperatures. Thus, the derivation of an exact, closed expression for the $P(T_K)$ is very nontrivial, even in RMT.

In RMT, for $\hbar T_K \ll 1$, one would expect the distribution of Kondo temperatures to be close to a Gaussian. The reasoning behind that is the following. In this limit one can go back to Eq. (2), expand the \tanh factor and find that T_K is given approximately by a sum of random variables (the wave function amplitudes). The central-limit theorem then ensures that a Gaussian distributed variable results from summing over independent random variables. However, as we show below, even for large $\hbar T_K \ll 1$ one finds a non-Gaussian behavior at the tails

of the distribution. This effect is shown to increase with disorder and is related to the appearance of local correlations between wave functions at different energies. It is therefore clear that in order to obtain the correct distribution of the Kondo temperature in random metals, it is crucial not to assume the random wave functions in Eq. (2) to be independent. Nevertheless, in order to simplify the discussion initially, we will start with this assumption in Sec. IV, where we will evaluate the distribution of T_K using the uncorrelated RMT (Porther-Thomas) distribution of wave functions. The effect of wave function correlations induced by disorder is left to Sec. VI.

III. CLEAN CASE

For later reference, let us briefly describe the behavior of the Kondo temperature in the clean limit. For that purpose, we assume a spectrum of N equally spaced levels, band width $D = N$, and spatially uniform wave function intensities (plane waves). When the Fermi energy is in the middle of the band and N is even, all levels are either doubly occupied or empty at $T = 0$ and we have $s_n = n - N/2$, $n = 1, \dots, N$. For $N = 1$ and $T_K = 0$, we then find for Eq. (1) the well-known solution

$$T_K^{(0)} = 0.57D \exp(-D/J) ; \quad (4)$$

which agrees to lowest order in $J=D$ with results from more accurate methods such as the numerical renormalization group. In fact, for the latter, the next leading order correction in the exponent has been found to be $-0.5 \ln(D/J)$,⁴ indicating that our treatment is valid for $J < D$ up to preexponential corrections. For small J , however, T_K approaches D and turns abruptly to zero at

$$J = \frac{D}{\ln(2N) + C} \quad (5)$$

in a nonanalytical fashion, namely,

$$T_K^{(0)}(J \neq 0) = \frac{1}{2 \ln[(D/J) + 1]} \quad (6)$$

(here $C = 0.58$ is the Euler number). For $J < D$, Eq. (1) has no solution in the clean limit. That means that the lowest order corrections to the bare exchange coupling remain weak down to zero temperature and marginal terms have to be included in order to determine T_K .⁴ Nevertheless, T_K is finite in this regime and we can conclude that there will be unscreened magnetic impurities (free moments) down to the lowest accessible temperatures in bulk clean metals when $J < D$.

IV. RANDOM MATRIX THEORY

In a disordered, phase-coherent metallic grain, the single-particle energy levels repel each other and the wave function intensities are distributed randomly. This behavior becomes very relevant to several physical properties of the system at low temperatures, namely, when $T < E_c$ (see Fig. 1).

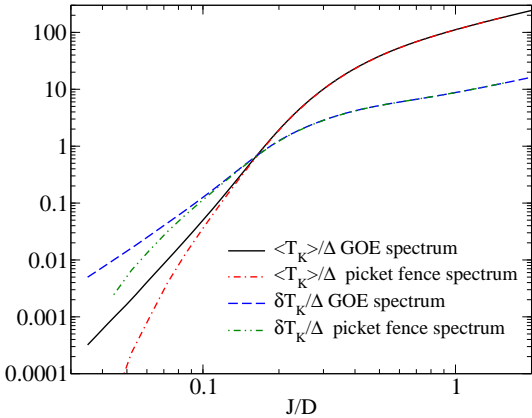


FIG. 2: (Color on-line) The dependence of the Kondo temperature average $\hbar T_K$ and standard deviation T_K on the exchange coupling J for unfolded GOE spectra ($N = 500$) as compared with those obtained for a spectrum of equally spaced energy levels (picket fence). In both cases wave function intensities were drawn from the Porter-Thomas distribution of Eq. (8), i.e., $\beta = 1$. It is only for $\hbar T_K \ll 1$ that the fluctuations of the energy levels result in an appreciable enhancement of $\hbar T_K$ and T_K .

For weak disorder, the dimensionless conductance parameter is very large: $g = E_c = 1$. In this regime, the spacing between consecutive levels within a window of energy ΔE obeys the Wigner-Dyson distribution of RMT.²² Moreover, within a given symmetry class, the wave function intensities x_n and the rescaled eigenenergies s_n fluctuate independently. The quantities x_n , $n = 1, \dots, N$ are themselves uncorrelated and obey the so-called Porter-Thomas distributions.^{19,23} For the Gaussian unitary ensemble (GUE - broken time-reversal symmetry class) and for the Gaussian orthogonal ensemble (GOE - time-reversal symmetric class) these distributions are given by

$$P_{GUE}(x_n) = \exp(-x_n) \quad (7)$$

and

$$P_{GOE}(x_n) = \frac{1}{\sqrt{2\pi}} \exp\left(-\frac{x_n^2}{2}\right); \quad (8)$$

respectively.

Using Eqs. (7) and (8) and substituting the delta function by its Fourier integral representation, we can perform the average over the wave function amplitudes in Eq. (3) exactly. For the orthogonal case, assuming an equally spaced spectrum, we obtain

$$P(T_K) = \frac{d}{dT_K} \sum_{r=1}^{N=2} \exp\left(-\frac{D G_r}{J}\right) \sum_{n=1, n \neq r}^{N=2} \frac{G_n}{G_r - G_n}; \quad (9)$$

where,

$$G_n = (n-1/2) \coth \frac{n-1/2}{2}; \quad (10)$$

Equation (9) can be further simplified in some limiting cases, as we will outline below.

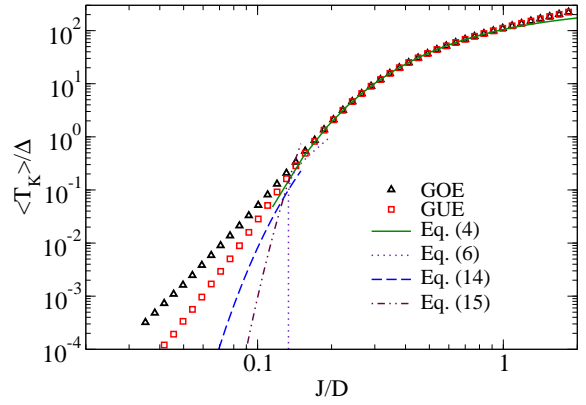


FIG. 3: (Color on-line) The dependence of average Kondo temperature on the exchange coupling for the GOE and GUE compared with the analytical solution in the clean case. The RMT data was averaged over 500 realizations for matrices of $N = 500$. Notice that randomness allows for solutions of Eq. (2) even at $J < J_c = 0.134$, a region inaccessible in the clean case. In this case the contributions to T_K come mainly from a few levels close to the Fermi energy, as a comparison with the results of the 2LS model, Eqs. (14) and (15), indicates.

In order to gain insight about the statistical properties of T_K over a wide range of values for J , we have solved Eq. (2) numerically using eigenenergies s_n obtained by diagonalizing GOE and GUE random matrices of size $N = 500$. The resulting semi-circular spectrum was unfolded into a flat band following standard procedures and the Fermi energy was set to the middle of the band ($E_F = 0$). Instead of using the random matrix eigenfunctions to get the local wave function intensities x_n , we generated these quantities directly from the Porter-Thomas distributions as given in Eqs. (7) and (8).²⁵ A total of 500 random matrix realizations were used for each ensemble type. For each realization (energy spectrum), we simulated different impurity locations by drawing 250 values of x_n , thereby increasing substantially the statistics of T_K without having to perform a large number of matrix diagonalizations.

The average and the standard deviation of the Kondo temperatures for GOE are shown in Fig. 2. They are compared with results obtained for an equally spaced spectrum, taking the eigenfunction intensities from the Porter-Thomas distribution as well. In Fig. 3, the GOE and GUE values of $\hbar T_K$ are plotted versus J together with the curves obtained in the clean, thermodynamic limit, namely, Eqs. (4) and (6). The average Kondo temperature is found to coincide with the clean case regardless of the ensemble symmetry when $\hbar T_K \gg 1$. It is only for $\hbar T_K \ll 1$ that it becomes dependent on the symmetry class. Note that fluctuations induce finite values for T_K even below the clean-limit threshold defined by Eq. (5).

From Fig. 2, it is clear that the average and standard deviation of the Kondo temperature are insensitive to level fluctuations when T_K is larger than 1 . Therefore, in that regime, the analytical result in Eq. (9), obtained by approximating the spectrum by a picket fence, should coincide with the numerical results obtained from Gaussian RMT ensem-

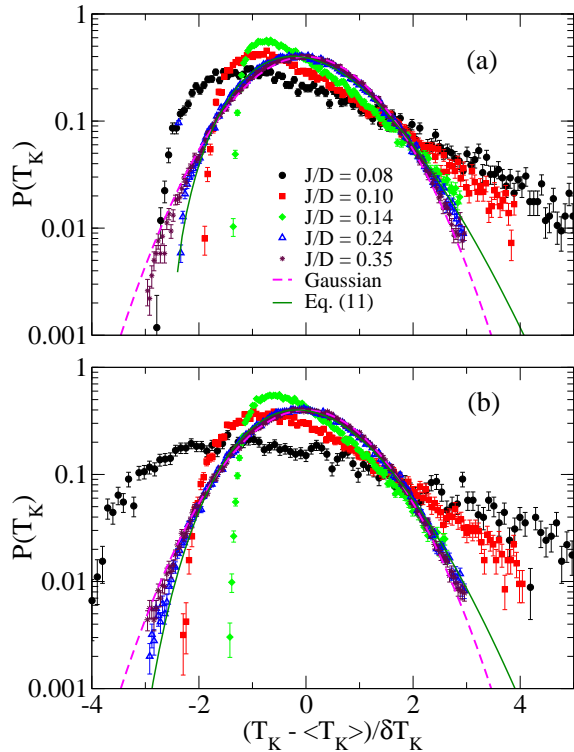


FIG. 4: (Color on-line) The GOE (a) and GUE (b) distributions of the Kondo temperature T_K for several exchange couplings J . Free moment events corresponding to the absence of $T_K > 0$ solution to Eq. (2) were excluded from the data. For small exchange couplings, a large portion of all events correspond to free moments, see Fig. (7). The dashed line represents a Gaussian with zero mean and unit variance. The solid line represents Eq. (11) for $J/D = 0.24$.

bles. For $T_K \rightarrow 0$, one can simplify Eq. (9) further, by setting $G_r = r^{-1/2}$ for $r > 0$ and $G_r = 0$ for $r < 0$. Thereby we obtain that the Kondo distribution has a stretched exponential form given by⁹

$$P(T_K) = \frac{1}{\pi} \exp^{-\frac{h}{2}} \ln \frac{e^{-\frac{h}{2}}}{e^{-\frac{h}{2}}}; \quad (11)$$

where $\tau_0 = T_K^{(0)} = \frac{1}{2}$. Notice that in the vicinity of $T_K^{(0)}$ the distribution is close to a Gaussian: For $\tau_0 \ll 1$ it can be approximated as

$$P(T_K) = \frac{1}{\pi} \exp^{-\frac{h}{2}} (T_K - \tau_0)^2 = 2 \tau_0; \quad (12)$$

near $T_K^{(0)}$. The departure from the Gaussian behavior occurs at the tails of the distribution: For $T_K \gg \tau_0$ ($T_K \ll \tau_0$) the curve defined by Eq. (11) runs below (above) a Gaussian. In Fig. 4, the numerical results for the distribution of Kondo temperatures for GOE and GUE spectra are shown for different values of J . The Kondo temperatures were shifted and rescaled in order to facilitate visualization and the comparison to a Gaussian distribution. The distribution becomes wider for small exchange couplings. Even for larger J , when the average hT_K exceeds τ_0 , there are marked deviations from

the Gaussian behavior, with distribution showing asymmetric non-Gaussian tails. There is good quantitative agreement between Eq. (11) and the numerical data for $J/D = 0.24$. However, this is not true for other values of J/D . This is mainly due to the relatively small size of the matrices used in the simulations, which makes the range of values of J where both $\tau_0 > 1$ and $J < D$ are satisfied too narrow.

Using the Gaussian approximation of Eq. (12), we can establish a relation between the standard deviation and the average of the Kondo temperature in the limit $T_K \rightarrow 0$, namely,

$$T_K = \frac{\sqrt{\tau_0}}{\sqrt{2}}; \quad (13)$$

where $hT_K \approx \tau_0$ is assumed. This analytical result has also been reported in Refs. 9,26,27. As shown in Fig. 5, Eq. (13) is only roughly consistent with the numerical simulations.

Since $T_K^{(0)}$ is ensemble independent in the $T_K \rightarrow 0$ limit, one finds from Eq. (13) that $T_K^{GOE} = T_K^{GUE} = \sqrt{\frac{1}{2}}$. When time-reversal symmetry is present ($J = 1$), level repulsion is weaker and the tendency to localization stronger. Consequently, the probability of having a vanishing wave function at the magnetic impurity position is enhanced, as well as the probability of large wave function splashes. This explains why the distribution is wider in this case than in the unitary case (broken time-reversal symmetry). Indeed, as shown in Fig. 6, the theoretical prediction for the ratio between the standard deviations of the Kondo temperature for the orthogonal and unitary ensembles is in quite good agreement with the results of the numerical simulations. For both RMT ensembles the distribution width scales with \sqrt{D} and therefore vanishes in the infinite volume limit. In Sec. VI we show that this is no longer true when there is a finite amount of disorder in the sample, such that spectral correlations beyond the Thouless energy scale exist.

Neither the distributions presented in Fig. 4 nor the average and the standard deviation used in the shifting and rescaling of T_K included free moment events, namely, those realizations where no solution with $T_K > 0$ could be found for Eq. (2). For small exchange couplings, the free moment events amount to a large portion of all events, which is why we plot them separately in Fig. 7. It is very remarkable that even for $J < J_c$, where $hT_K \approx \tau_0$, the distribution shows a clear maximum at a finite value of T_K . The distribution decays towards $T_K = 0$ even though there is a large amount of free moments in this case (see Fig. 7). This peculiar behavior can be qualitatively understood by recalling the level repulsion of RMT ensembles and can be quantitatively treated within a two-level model, as outlined in Sec. V.

V. TWO-LEVEL SYSTEM APPROXIMATION

For $T_K < \tau_0$, only the two states closest in energy to the Fermi energy are appreciably coupled to the magnetic impurity. For small exchange couplings $J < J_c$, this affects the

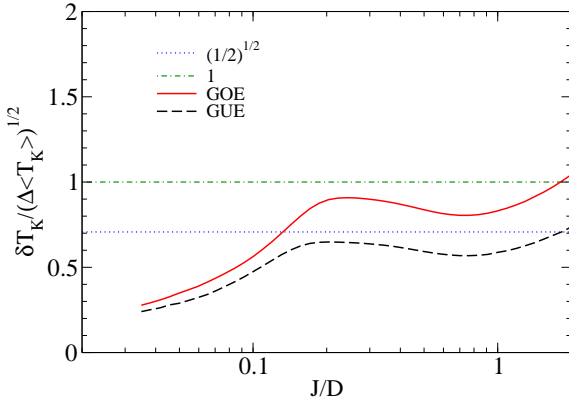


FIG. 5: (Color on-line) The Kondo temperature average $\hbar T_K$, standard deviation T_K , and the ratio $T_K = (\hbar T_K)^{1/2}$ as a function of the exchange coupling constant J for the GOE and GUE ensembles.

whole distribution of Kondo temperatures, while for larger exchange couplings it applies only to the small- T_K tail. In this limit, we can simplify the analytical calculations by separating the contributions to the sum in Eq. (2) into two groups. In the first we include only the two nearest levels to the Fermi energy and fully take into account the fluctuation of their relative spacing and their wave function amplitudes. The remaining levels form the second group and are treated assuming an equally spaced spectrum and $x_n = 1$. When the wave functions at the Fermi level are distributed according to the GOE Porter-Thomas distribution but the energy levels are kept fixed, the average Kondo temperature is found to be

$$\hbar T_K \text{ i}_{\text{GOE}} = \frac{Ei(-1=2)}{2e} \exp \left(\frac{D}{J} + \frac{D}{J} \right) ; \quad (14)$$

where $Ei(x)$ denotes the exponential integral function,²⁸ with $Ei(-1=2) = 0.56$. For the GUE Porter-Thomas distribution, we obtain instead

$$\hbar T_K \text{ i}_{\text{GUE}} = \frac{2Ei(-1=2)}{e^2} \exp \left(\frac{2D}{J} + \frac{2D}{J} \right) ; \quad (15)$$

showing that the average Kondo temperature in the unitary ensemble becomes exponentially smaller than in the orthogonal ensemble, which is consistent with the numerical result presented in Fig. 6.

It is of particular interest to determine the probability of having unscreened, free magnetic moments in the system for a given bare exchange coupling, $P_{\text{free}}(J)$. This function is equal to the probability that the Kondo temperature is either zero or that there is no solution to Eq. (2). In these cases, the correction to the exchange coupling remains small for all temperatures and the Kondo effect is quenched, in the sense that the magnetic moment remains unscreened down to zero temperature. As discussed in Sec. III, in the clean limit the free moment probability is a sharp function of J , namely, $P_{\text{free}}(J = J_c) = 1$, and $P_{\text{free}}(J > J_c) = 0$, with J_c given by Eq. (5). When there is randomness, J is a function of the random wave function intensities x_n and level spacings s_n of

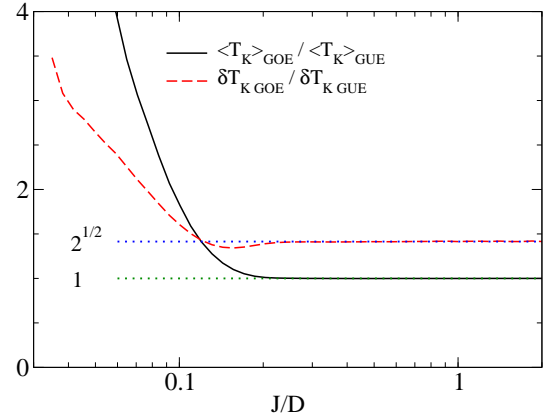


FIG. 6: (Color on-line) The ratios between the GOE and GUE values for $\hbar T_K$ and for T_K . Analytical considerations predict these ratios to yield universal numbers, 1 and $\sqrt{2}$, respectively, over a wide range of exchange couplings $J > J_c$. Deviations from this behavior are seen for smaller exchange couplings only, when $J < J_c$. These can be attributed to fluctuations of the two levels closest to the Fermi energy.

the closest levels to the Fermi energy. Upon averaging over their distributions, we expect the step function to become a smoothly decaying function. Thus, due to the finite probability that level spacings at the Fermi energy exceed Δ or wave function intensities are small, there is a finite probability of finding free moments even at $J < J_c$, where the magnetic moment would be screened without randomness. We have determined this probability distribution numerically (see Fig. 7). For $J < J_c$, we can compare it with the result obtained within a 2LS approximation. A first attempt can be made by setting the wave function amplitudes to be constant, $x_1 = 1$ and fixing all but the two closest levels to the Fermi energy, which are allowed to fluctuate according to the Wigner surmise.²² For the GOE we obtain

$$P_{\text{free}}(J) = \exp \left(\frac{D = J}{D = J + 2)^2} \right) ; \quad (16)$$

which is valid only for $J < J_c = J_c = (1 - J_c = D)$, since for larger values of J the fluctuations of the other levels can no longer be neglected.

When the wave function amplitudes are constant, the probability to have free magnetic moments is just proportional to the probability that the level spacing at the Fermi energy is of the order of $T_K^{(0)}(J)$. That is exponentially small for $J > J_c$. However, in Fig. 7 we see that the decay with J is slower than that, indicating that the fluctuations of wave functions are crucial. Indeed, in principle there is no appealing reason for taking $x_1 = 1$ under realistic conditions. When wave functions are allowed to fluctuate according to the Porter-Thomas-distribution, we rather obtain (again for the GOE)

$$\begin{aligned} P_{\text{free}}^{\text{GOE}}(J) &= \int_0^{\infty} dx \exp \left(-x \frac{x^2}{4u_J^2} \right) \\ &= u_J \exp \left(\frac{u_J^2}{4} \right) E \text{rfc} \left(\frac{u_J}{2} \right) ; \quad (17) \end{aligned}$$

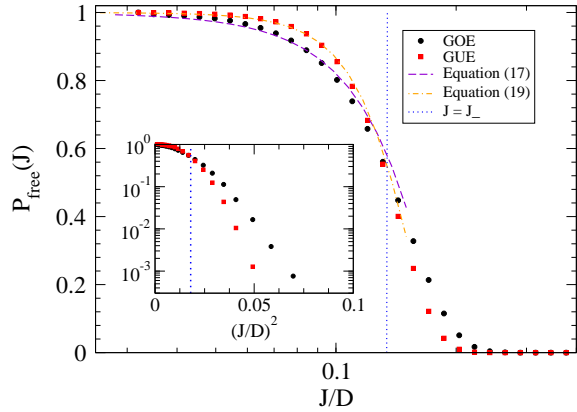


FIG. 7: (Color on-line) Probability of finding free magnetic moments. The data points correspond to the fraction of events in the RMT simulations where either $T_K = 0$ or no solution to Eq. (2) was found, and is plotted as a function of the exchange coupling J . The dotted line indicates the point where $J = J_c$. There is a good agreement between simulations and the analytical predictions for $J < J_c$ based on the two-level system model. The inset shows the tail of the probability function at $J > J_c$.

with

$$u_J = 1 + \frac{D}{2J} - \frac{D}{2J} : \quad (18)$$

Note that $P_{\text{free}}^{\text{GOE}}(0) = 1$ and $P_{\text{free}}^{\text{GOE}}(J_c) = 2 = 1$. For $J > J_c$, the fluctuations of the other energy levels become important and the 2LS approximation can no longer be used. Similarly, for the GUE we obtain

$$P_{\text{free}}^{\text{GUE}}(J) = 1 - \frac{4}{\pi^2} \int_0^{J_c} dx x^2 (1 + u_J x) \exp(-u_J x - \frac{x^2}{4}) : \quad (19)$$

These results are compared to the numerical calculations in Fig. 7 and good agreement is found for $J < J_c$. Thus, in RMT, we can conclude that fluctuations of wave functions do enhance the probability of finding free moments for $J > J_c$. It is then natural to ask whether this tendency continues when we go beyond the RMT domain. In Sec. VI, we will address this question in the context of a metallic grain where the disorder parameter can be tuned.

VI. DISORDERED METALS

In order to investigate the effect of nonmagnetic disorder on the statistical fluctuations of the Kondo temperature, we use a tight-binding model with nearest-neighbor hopping and random site potential to describe the conduction electrons,

$$H = \sum_{\langle i,j \rangle} \frac{x}{t} c_i^\dagger c_j + h.c. + \sum_{i=1}^N V_i c_i^\dagger c_i ; \quad (20)$$

where each site potential V_i is drawn from a flat box distribution of width W centered at zero. We assume each eigenstate of H to be spin degenerate, therefore sums over spins are implicit in Eq. (20). We consider only square lattices with periodic boundary conditions. Using standard numerical techniques, we have diagonalized the Hamiltonian H for a large set of realizations of the disordered potential. The resulting eigenenergies E_n and eigenvectors $\psi_n(i)$, $n = 1, \dots, N$, were used in conjunction with Eq. (1) to determine T_K for each of the disordered potential realization. In all simulations the Fermi level was placed at the lower quarter of the band in order to avoid the large peak in the density of states at $E = 0$, reminiscent of the van Hove singularity found in the clean limit. No unfolding of energy levels was used. The simulations were carried out for 20×20 square lattices. The number of realizations varied from 100 to 4,000, depending on the disorder strength. No magnetic flux was included, thus all results refer to the time-reversal symmetric class.

A connection between the tight-binding disorder strength W and the dimensionless parameter g can be made by recalling the expression for the nonmagnetic scattering rate in Born approximation,

$$\frac{1}{\tau} = 2 \pi V^2 ; \quad (21)$$

where $\tau = 1 = L^2$ (we set the lattice constant $a = 1$, therefore $N = L^2$). Noting that $V^2 = W^2 = 12$ and $\tau = 8t = N$, we obtain

$$\frac{1}{\tau} = \frac{W^2}{48} : \quad (22)$$

Defining the dimensionless parameter $g = E_F \tau$ and setting $E_F = 2t$, we arrive at

$$g = \frac{3}{2} \frac{8t}{W}^2 : \quad (23)$$

It is important to remark that Eq. (23) does not provide the dimensionless conductance parameter. Nevertheless, g here conveniently characterizes the strength of the disorder potential. Moreover, Eq. (21) is valid only in the perturbative sense, when disorder is not too strong, and should break down near $g = 1$. Furthermore, when deriving Eq. (22) we assumed a flat density of states (i.e., a parabolic dispersion relation), which is a rough approximation. Thus, g , as calculated in Eq. (23), has to be considered merely as a way to parametrize the transition from a metallic ($g = 1$) to a strongly disordered, localized regime ($g < 1$).

The dependence of the average Kondo temperature on g is shown in Fig. 8 for several exchange coupling strengths. For each J , the data was normalized by the average Kondo temperature at $g_0 = 3.4$ ($W = 3t$) to facilitate the visualization. Note that $\langle T_K \rangle$ depends only weakly on disorder, as long as $g < 1$. In the metallic regime, the Kondo temperature only becomes smaller than the level spacing only at very weak exchange couplings, $J < J_c$, as shown in the inset of Fig. 8. The average Kondo temperature is only substantially affected by disorder when localization sets in ($g < 1$). This behavior

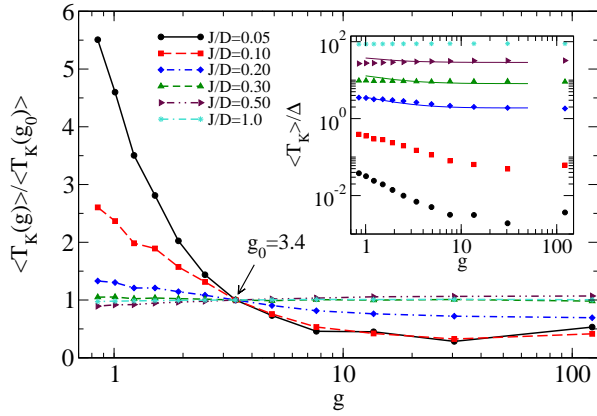


FIG. 8: (Color on-line) The dependence of the average Kondo temperature hT_K on the disorder parameter g for a 20×20 lattice and different values of J . To facilitate the comparison, hT_K was divided by its value at $g_0 = 3.4$ ($W = 3t$). Inset: Same data without the normalization, together with the prediction based on Eq. (33) and taking into account the finite values of E_c and Δ ($J=D = 0.20, 0.30$, and 0.50 only).

is reminiscent of the independence of the critical temperature on nonmagnetic disorder in a conventional superconductor.²⁹

In Fig. 9 we present the dependence of standard deviation T_K on the exchange coupling and the dimensionless conductance (inset). There is good agreement between the GOE and the weak disordered case for a wide range of values of $J < D$.³⁰ As the disorder is increased, fluctuations in the Kondo temperature increase in amplitude.

In order to have a better understanding of the behaviors shown in Figs. 8 and 9, we derive analytical expressions for the average and the standard deviation of the Kondo temperature in the metallic regime but beyond RMT by taking into account wave function correlations. To this end, we recall that the local density of states (LDOS) is defined as

$$\langle r; E \rangle = \sum_{n=1}^N j_n(r) j_n^* (E - E_n) : \quad (24)$$

We also make use of the well-known correlation function of local density of states (LDOS), as defined by

$$\begin{aligned} R_2(r; !) &= h(r; E) \langle r; E + ! \rangle i \\ &= \frac{1}{2} \sum_{n \neq m} j_n(r) j_n^* j_m(r) j_m^* (E - E_n) \\ &\quad (E + ! - E_n) i : \end{aligned} \quad (25)$$

It is convenient to separate diagonal from off-diagonal terms in Eq. (25). The correlation function of LDOS can then be rewritten in terms of the spectral correlation function $R_2(!)$,

$$\begin{aligned} R_2(r; !) &= R_2(!)^2 j_n(r) j_n^* j_m(r) j_m^* j_{n=E_n, m=E_m} \\ &\quad + (! =)^2 j_n(r) j_n^4 : \end{aligned} \quad (26)$$

For $! < E_c$, the function $R_2(!)$ is an oscillatory decaying function with corrections of order $1=g^2$ to the leading RMT

term. For the time-reversal symmetric case ($= 1$), it reads

$$\begin{aligned} R_2(s = \frac{!}{h}) &= 1 - \frac{\sin^2(s)}{2s^2} \\ &\quad + \frac{1}{2} \operatorname{sgn}(s) \operatorname{Si}(s) \frac{i}{s} \frac{\cos(s)}{s} - \frac{\sin(s)}{(s)^2} \\ &\quad + \mathcal{O}(1=g^2); \end{aligned} \quad (27)$$

where, $\operatorname{Si}(z) = \int_0^z dy \sin y = y$.²³ For frequencies exceeding the Thouless energy, $! > E_c$, the oscillatory part of the spectral correlation function decays exponentially, while there is a correction of order $1=g^2$ which decays as $1=s$ without oscillations.²³ While for pure RMT there are no correlations between wave functions at different energies, in the disordered Anderson model these correlations are of order $1=g$, namely,²³

$$j_n(r) j_m(r) j_{n=E_n, m=E_m} = 1 + \frac{2}{R} \operatorname{e}(!) \quad (28)$$

for $n \neq m$, while

$$j_n(r) j_n^4 = 1 + \frac{2}{1 + \frac{2}{R} \operatorname{e}(0)} : \quad (29)$$

These analytical results have recently been confirmed numerically in Ref. 24. Notice that the correlation is stronger when time-reversal symmetry is present, $= 1$. The dependence on the disorder enters through the summation over diffuson modes, which is here represented by

$$(!) = \sum_q \frac{1}{D_e q^2 - i!} : \quad (30)$$

In two dimensions (2D) and for $L > 1$, we obtain²³

$$(2D) (!) = \frac{1}{2g} \ln \frac{1=L^2}{1=L^2} \frac{i!=D_e}{i!=D_e} ; \quad (31)$$

with $1=L=v_F$ and $D_e=v_F L=2$:

Since the Kondo temperature is defined by a sum over all eigenstates in the band, fluctuations of wave function amplitudes at the position of the magnetic impurity add up quite effectively when the wave functions are correlated over a large energy range. These correlations are nonzero over an interval of the order of the elastic scattering rate $1=\tau$. Thus, one can expect that fluctuations of the Kondo temperature can exist even in the thermodynamic limit, when both τ and E_c vanish.

Defining $T_K^{(0)}$ as the Kondo temperature in the absence of LDOS fluctuations and introducing Eq. (24) into (1), one finds³¹

$$T_K = T_K^{(0)} \exp \int_{E_F}^Z \frac{dE}{2E} \frac{(r; E_F + E)}{2E} \tanh \frac{E}{2T_K} ; \quad (32)$$

where $\tau = \frac{h}{T_K^{(0)} \operatorname{e}(0)}$. Expanding the exponent to second order in τ and ensemble averaging, we arrive at

$$\begin{aligned} hT_K i &= T_K^{(0)} \frac{1 + S}{1 + S} ; \quad ; T_K^{(0)} + V ; E_c ; T_K^{(0)} \\ &\quad + Q ; E_c ; T_K^{(0)} : \end{aligned} \quad (33)$$

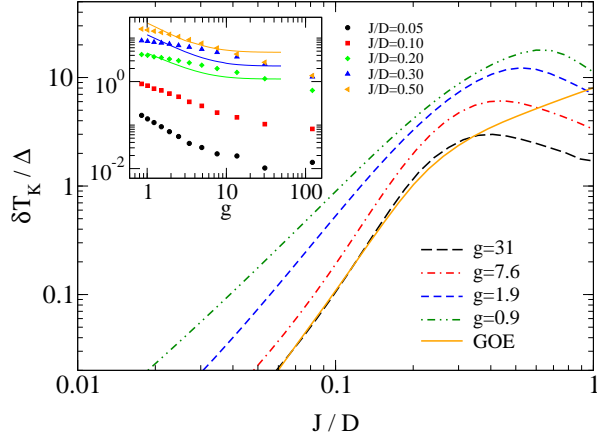


FIG. 9: (Color on-line) The standard deviation of the Kondo temperature as a function of the exchange coupling for the disordered tight-binding model and a 500 500 GOE. Inset: Dependence on the dimensionless disorder parameter, together with the prediction based on Eq. (34) for the cases $J/D = 0.20, 0.30$, and 0.50 .

and

$$(\langle T_K \rangle)^2 = \frac{h}{2} \frac{T_K^{(0)} i_2 h}{T_K^{(0)} S} ; \quad ; T_K^{(0)} + V ; E_c, T_K^{(0)} + Q ; E_c, T_K^{(0)} ; : \quad (34)$$

The function S arises from the spectral self-correlation term ($!=$) and is given by

$$S(\langle ; ; T_K \rangle) = \frac{1}{8} \left(1 + \frac{2}{Z_D E_F} \right) \left(1 + \frac{2}{E_F^2} \text{Re}(\langle 0 \rangle) \right) \frac{dE}{E^2} \tanh^2 \frac{E}{2T_K} ; \quad (35)$$

This term is of order $=T_K$ and therefore vanishes in the thermodynamic limit as $! 0$. The decaying part of the spectral correlation function yields the term

$$V(\langle ; E_c ; T_K \rangle) = \frac{1}{8} \frac{Z_D E_F}{E_F} \frac{dE}{E} \frac{dE^0}{E^0} \tanh \frac{E}{2T_K} \tanh \frac{E^0}{2T_K} \left[R_2(E - E^0) - 1 \right] \frac{2}{1 + \frac{2}{E_F^2} \text{Re}(\langle E - E^0 \rangle)} ; \quad (36)$$

In 2D, $R_2(!) - 1$ decays as $1!=!$ for frequencies exceeding the Thouless energy. Hence, it causes V to have a nonvanishing term as $E_c ! 0$, but this term turns out to be only of order $1=g^2$. If correlations of wave functions are taken into account only up to first order in $1=g$, V can be discarded. At finite E_c , however, it needs to be taken into account since it yields terms of order $E_c=T_K$ due to spectral correlations at small frequencies, $! < E_c$.

The term arising purely from the correlations of wave func-

tions is given by

$$Q(\langle ; E_c ; T_K \rangle) = \frac{1}{4} \frac{Z_D E_F}{E_F} \frac{dE}{E} \frac{dE^0}{E^0} \tanh \frac{E}{2T_K} \tanh \frac{E^0}{2T_K} \text{Re}(\langle E - E^0 \rangle) ; \quad (37)$$

This term survives the thermodynamic limit. For instance, in 2D,

$$\text{Re}(\langle 2D \rangle(!)) = \frac{1}{4g} \ln \frac{1+4^2 + !^2}{E_c^2 + !^2} ; \quad (38)$$

For $1=g=T_K$, one can use Eq. (38) with $E_c = 0$ to write the double integral in Eq. (37) in terms of polylogarithm functions. To leading order and after setting $E_F = D = 2$, we obtain

$$Q^{(2D)}(\langle ; 0 ; T_K \rangle) = \frac{1}{g} \ln \frac{E_F}{g T_K} ; \quad (39)$$

which is valid when $E_F = T_K$ and $g = 1$. Combining Eqs. (34) and (39), we find that

$$T_K \frac{i_{2D}}{T_K^{(0)}} \frac{1}{g} \ln \frac{1}{T_K^{(0)}} ; \quad (40)$$

This means that the width of the distribution of Kondo temperatures remains finite as $! 0$ even in the metallic regime ($g = 1$). In the same limit, the average of the Kondo temperature is found to increase with the disorder as

$$hT_K \frac{i_{2D}}{T_K^{(0)}} < \frac{1}{1 + \frac{c}{g}} \ln \frac{1}{T_K^{(0)}} ; \quad (41)$$

where the constant c depends on the exact positioning of the Fermi energy. Putting the Fermi energy in the middle of the band, we find $c = 1=6$, was previously reported in Ref. 9. While this effect is only of order $1=g$, it is enhanced by the large factor of third power in the logarithm of $T_K^{(0)}$. Repeating the calculations using the diffusion propagators for quasi-one-dimensional wires, this enhancement is found to be even of order $1=\frac{p}{g}$, as previously reported in Ref. 46, where the asymptotic result in 2D, Eq. (40) has been obtained as well. Thus, we can conclude that the Anderson theorem, which states that the critical temperature of superconductors is not affected by nonmagnetic disorder, up to small corrections of order $1=g$, has no analog for low-dimensional disordered Kondo systems, contrary to what has been proposed in Ref. 32.

The full expressions for $hT_K i$ and T_K , including the dependences on g and E_c , Eqs. (33) and (34), are compared to the numerical data in Figs. 8 and 9, respectively. The analytical expressions do capture the qualitative aspects correctly and are in reasonable quantitative agreement in their regime of applicability, namely the metallic diffusive regime, $1 < L < 20$ (for $L = 20$, that interval corresponds to $1 < g < 30$).

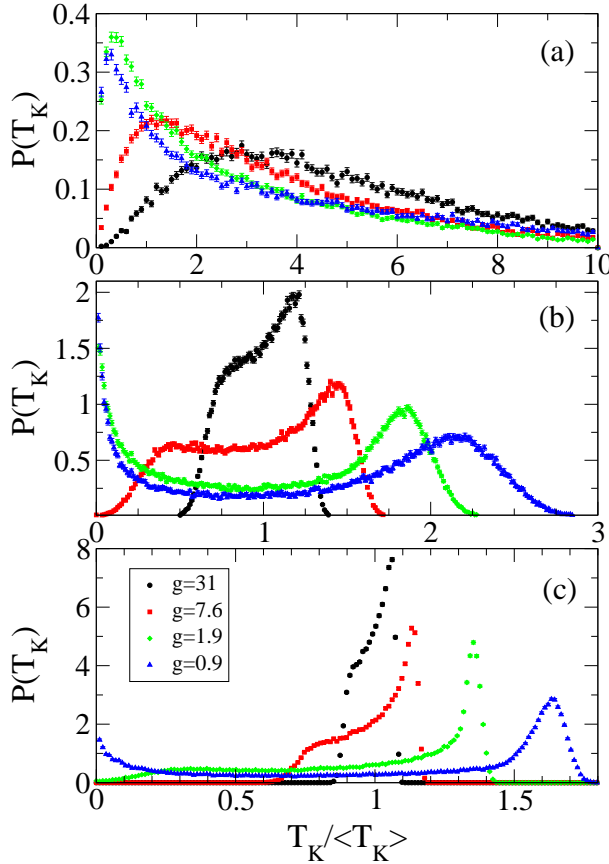


FIG. 10: The distribution of the Kondo temperature for the Anderson model on a 20 × 20 square lattice without magnetic field (solid symbols) and for the GOE with $N = 400$ (dashed line). The Fermi level was set to the 1/4 band position. The exchange coupling relative to the full band width, $J=D$, take the values: (a) 0.1, (b) 0.35, and (c) 0.6. Events corresponding to $T_K = 0$ fall outside the vertical scale in (a). 4,000 realizations were used for each value of g .

There is an enhancement of the Kondo temperature and an increase of its variance as the disorder strength increases and g decreases. According to the analytical calculations, this is mainly due to the appearance of weak correlations of wave functions at different energies. Albeit weak in the metallic regime, these correlations have a sizeable effect on the Kondo temperature. That is because the Kondo temperature involves a summation over all eigenstates with a finite wave function amplitude at the location of the magnetic impurity. As one moves from the diffusive to the localized regime, an increase in correlations of the LDOS at different energies is expected to induce even stronger fluctuations in the Kondo temperature.

The distribution of Kondo temperatures also changes drastically as function of disorder strength and exchange coupling amplitudes. This can be observed in Fig. 10, where we show the distributions obtained from the numerical simulations of the disordered tight-binding model. Even for weak disorder and large exchange coupling ($J = J$) there are strong deviations from the Gaussian and RMT behaviors, with a bimodal structure appearing. Two distinct peaks are clearly visible when $J=D$ is not too small. As $J=D$ increases, weight is

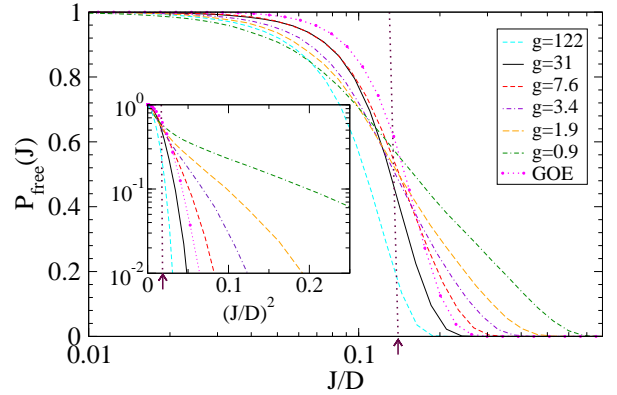


FIG. 11: Probability of finding free moments as a function of the exchange coupling for the Anderson model at different disorder strengths. Also shown is the curve for the GOE and the the clean case lower bound $J = J$ (marked by an arrow). Inset: the same curves in a linear-log scale.

transferred from the low- T_K to the high- T_K peak [see Fig. 10 (c)]. The distributions never come close to Gaussian, as they do in the RMT case. Since Eq. (39) indicates that the enhancement of fluctuations in the Kondo temperature should survive the thermodynamic limit, we believe that the overall form observed in Fig. 10, with a wide plateau in $P(T_K)$ for weak disorder and a marked second peak at small T_K for strong disorder, should survive as the finite size L of the lattice is increased. However, in order to check this statement numerically one would need to perform a finite-size scaling analysis. For an analytical proof, at least a few moments higher than the variance would have to be calculated. Both are beyond the scope of this paper and will be investigated in future work. However, it is important to remark that in the strong disorder limit, a finite-size scaling analysis has already been performed in Ref. 33. It was found that a critical feature seen in Figs. 10 (b) and (c), namely, the divergence of the distribution as $T_K \rightarrow 0$ at strong disorder, does survive finite-size scaling. In Ref. 33, this divergence was found to be a power law that depends on the space dimension.

It is worth remarking that the events corresponding to $T_K = 0$ are not shown in Fig. 10 but they were taken into account in the evaluation of $\hbar T_K$ and T_K . The long tail toward the small- T_K region indicates that disorder enhances the probability of having unscreened, free magnetic moments at zero temperature. This is confirmed in Fig. 11, where we show the probability of finding no solution to Eq. (1), $P_{\text{free}}(J)$, as a function of $J=D$. When disorder is weak, the curves are very similar to those obtained in the GOE case. They resemble smoothed step functions with the turning point approximately at the clean-case lower bound J . (One should note that the band widths are not exactly the same for different disorder strengths, thus the termination points should vary slightly between different data sets.) When one moves away from the diffusive regime and into the strongly localized regime ($g < 1$), the probability of finding free moments at $J = J$ is strongly enhanced.

VII. DEPENDENCE OF $P(T_K)$ ON THE CONCENTRATION OF MAGNETIC IMPURITIES

In the absence of an external magnetic field, the symmetry class of the underlying single-particle basis to the Kondo problem is controlled by the concentration of magnetic impurities and the relation between certain energy scales. The general idea is that, as the number of magnetic impurities increases, statistical fluctuations of the electron states in the grain cross over from the orthogonal class (time-reversal symmetric) to the unitary class (broken time-reversal symmetry). This is due to the fact that the spin dynamics of the magnetic impurities can be slow compared to the time scale of the conduction electrons, thereby breaking effectively the time-reversal invariance on their time scale.^{34,35} However, as we will argue below, the dynamical regime in the grain, and consequently the strength of the Kondo screening, also plays a crucial role in determining on which side of this crossover the system finds itself.³⁶

We begin by recalling that for a mesoscopic sample in the weak localization (WL) regime, i.e., at energies $E > E_c$ (short time scales), the dimensionless parameter controlling the orthogonal-unitary crossover due to magnetic impurities can be written as³⁴

$$X_s^{WL} = \frac{1}{E_c s}; \quad (42)$$

with the crossover centered at $X_s = 1$. As the energy is lowered below E_c (long time scales), one enters the zero-dimensional, RMT regime, where the average level spacing

takes over E_c as the relevant energy scale. In that regime, the crossover parameter is given by

$$X_s^{RMT} = \frac{1}{s} = g X_s^{WL} \quad (43)$$

instead. Thus, for a sample in the RMT regime, the crossover occurs for spin scattering rates smaller by a factor $1=g$ with respect to the weak-localization regime. This crossover in the RMT regime has been recently studied for a Kondo quantum dot in an Aharonov-Bohm ring.³⁷

At any finite temperature, the spin scattering rate $1=s$ is renormalized by Kondo correlations: It is small at both $T=T_K$ and $T=T_K$, having a maximum at around $T=T_K$, as has been observed in weak-localization experiments.^{38,39} This behavior is analogous to that observed in the reentrance of gapless superconductivity.⁴⁰ For a clean sample, one finds that⁴⁶

$$\frac{1}{s(T)} = \begin{cases} \gtrless \frac{n_m s(s+1)}{n_m}; & T > T_K; \\ \gtrless \frac{n_m}{T_K} \frac{2}{16} \frac{w^2}{4} c_{FL}; & T < T_K; \end{cases} \quad (44)$$

where n_m is the density of magnetic impurities, s denotes their spin, w is a numerical factor smaller than unit, and $w=0.41$ is the Wilson number. In Ref. 46, it was found numerically that $w=0.2$. In Eq. (44), c_{FL} is a factor that arises from the relation between the inelastic scattering rate and the temperature-dependent dephasing rate.⁴⁶ In 2D, $c_{FL}=0.946$.

Before we proceed with our discussion, a few remarks about Eq. (44) are necessary. First, the spin scattering rate is defined as in Ref. 34, which is by a factor 1/2 smaller than the dephasing rate, as defined in Ref. 46. Secondly, note the difference in definition of our T_K with respect to that used in Ref. 46: Ours corresponds to their *perturbative* T_K . Thirdly, the numerical prefactor of the $(T=T_K)^2$ term in Eq. (44) was obtained within Fermi liquid theory,¹ where the exact result differs from that obtained in the standard Sommerfeld low-temperature expansion by a factor 3. In the following, we will approximate the numerical prefactor multiplying the $(T=T_K)^2$ term by unit, since $w^2/4 c_{FL}=16=0.968$.

The low-temperature limit of the spin scattering rate shows the expected Fermi-liquid scaling based on Nozieres' theory for the Kondo problem, which is valid at $T \ll T_K$.^{3,41} At temperatures exceeding T_K , Eq. (44) is consistent with the perturbative poor man's scaling.^{2,18,40,42,43} However, we note that recent experiments have shown the scattering rate to be approximately linear with temperature for a wide interval below T_K .⁴⁴ This behavior has been explained theoretically by Zarand and coworkers⁴⁵ in a numerical renormalization group calculation of the frequency-dependent inelastic scattering rate, where they also obtained $w=0.2$.

In principle, one could expect that the maximum value that $1=s$ can reach should be given by the unitary limit of the scattering cross section. However, in reality, the maximum value is found to be smaller than that by the factor w shown in Eq. (44). In 2D,⁴⁵

$$\frac{1}{s_{max}} = \frac{n_m}{N_m}; \quad (45)$$

Thus, the maximal value the crossover parameter can reach for a two-dimensional sample in the weak localization regime is

$$X_s^{WL}_{max} = \frac{N_m}{g}; \quad (46)$$

where $N_m = n_m L^2$ is the number of magnetic impurities for a sample with linear size L . When there are only a few magnetic impurities, $N_m < g$, the crossover parameter is small and the sample is in the orthogonal regime. Increasing the concentration of magnetic impurities increases the parameter X_s and eventually leads to the unitary regime. As found in Sec. IV, this is accompanied by a decrease in the width of the distribution of Kondo temperatures.

It has recently been pointed out that the correlations between wave functions at different energies are enhanced in the GOE-GUE crossover regime.⁴⁷ Thus, since the width of the distribution of the Kondo temperature is enhanced by wave function correlations, one can expect⁴⁸ a widening of the Kondo distribution in the GOE-GUE crossover regime due to the presence of a weak magnetic field or a small amount of spin scattering. The wave function correlation function is then given by

$$\langle j_n(r) j_m(r) \rangle_{E_n, E_m} = \frac{2}{4} \frac{2}{4-2} + \frac{2}{2!} \frac{2}{2!}; \quad (47)$$

Here, γ is related to the magnitude of the time-reversal breaking perturbation. In the presence of an external magnetic field B , $\gamma^2 = 1 = \gamma_B$, where γ_B is the magnetic phase-shift rate. For a diffusive quantum dot, this rate is given by $\gamma_B = e^2 D_e B^2 L^2 = h^2$, where D_e is a geometrical factor of order unity. In the presence of magnetic impurities, the GOE-GUE crossover is governed by the spin scattering rate and $\gamma^2 = 1 = \gamma_s$. Remarkably, the mixing of GOE-eigenfunctions brought by time-reversal symmetry breaking induces wave function correlations over a macroscopic energy scale either equal to $1 = \gamma_B$ or $1 = \gamma_s$. However, the amplitude of these correlations is proportional to γ_s and therefore they vanish in the thermodynamic limit.⁴⁷ In order to see that, we use Eq. (32) to explicitly evaluate the width of the distribution of the Kondo temperature related to the crossover wave function correlations. We obtain

$$T_K^{(0)} = 2 \int_0^{\infty} \frac{dt}{t} \ln \frac{1+t}{1-t} : \quad (48)$$

Thus, for $T_K^{(0)} = 1 = \gamma_s$, these GOE-GUE correlations only contribute to a width $T_K^{(0)} = \frac{1}{\gamma_s} = \frac{1}{\gamma_B}$ that vanishes in the thermodynamic limit when $\gamma_B \neq 0$, but is larger than the value obtained in the pure RMT ensembles by a factor $\frac{T_K^{(0)}}{\gamma_s}$.

As the magnetic impurity concentration increases further, the superexchange interaction between magnetic impurities begins to compete with the Kondo screening.⁴⁹ The superexchange interaction coupling J_{KKY} fluctuates and its average and spreading depend on the amount of disorder, impurity concentration, and details of the Fermi surface. In the spin-glass phase, J_{KKY} is zero on average,⁵¹ but fluctuates according to a wide log-normal distribution.⁵² Its typical value is of the same order as that of a clean sample,⁵³ namely, $\langle J_{KKY}^2 \rangle = (n_m = 1) (J=D)^2 \cos(2k_F R)$. Even when the typical superexchange coupling constant is smaller than T_K , there is a small chance that clusters of spins form. When two localized spins couple ferromagnetically to form a triplet state, they contribute to the dephasing rate of itinerant electrons. Such a contribution to the dephasing rate scales with n_m^2 .^{46,54} When J_{KKY} exceeds the Kondo temperature T_K of a single magnetic impurity, the spins of the magnetic impurities are quenched. They form a classical random spin array whose spin scattering rate is smaller than that for free quantum spins by the factor $1=3$, and scale linearly with n_m .⁵⁰ At intermediate concentrations of magnetic impurities Griffiths-McCoy singularities can appear and induce an interesting though more complex behavior (see Ref. 55 for a review).

VIII. DEPHASING DUE TO FREE MAGNETIC MOMENTS IN DISORDERED METALS

We now discuss the relevance of the distribution of the Kondo temperature T_K to the quantum corrections of the conductance of mesoscopic wires.

As discussed in Sec. VII [see Eq. (44), in particular], the temperature dependence of the spin scattering rate has a max-

imum at T_K , resulting in a plateau of the dephasing time.^{38,39} However, we have found in Sec. VI that disorder can result in a finite probability of having magnetic impurities with vanishingly small Kondo temperatures. Thus, the question arises whether the latter effect can yield a finite contribution to the dephasing rate at temperatures below the average Kondo temperature. It has recently been argued that the dephasing rate due to a magnetic impurity can be related to the inelastic cross section of a magnetic impurity at the Fermi energy:^{45,46}

$$\frac{1}{\gamma} = n_m v_F \text{inel} : \quad (49)$$

where v_F is the Fermi velocity, and the inelastic cross section can be obtained from the difference between the total and the elastic cross section,

$$\text{inel}(\mathbf{E}_F) = \text{total} - \text{el} : \quad (50)$$

Using the optical theorem, both the total and the elastic cross sections can be related to matrix elements of the T-matrix of the magnetic impurity.⁴⁵ Based on the fact that in the derivation of the weak-localization correction one averages over the disorder potential and thereby recovers translational invariance, the authors of Refs. 45 and 46 calculated the spin scattering rate of Eq. (49) for a plane waves basis. However, one should calculate the spin scattering rate as averaged over all momentum directions in order to correctly determine how the dephasing rate caused by magnetic impurities is affected by the random environment. Following this approach, we find that the spin scattering rate of a state of energy E should be given by⁵⁶

$$\begin{aligned} \gamma_s(E; T) = & \frac{n_m}{\pi} \int_{E_p}^{\infty} \frac{h}{E - E_p - i\Gamma_p} \text{Im} \frac{h}{\Gamma_p} \frac{1}{\Gamma_p} \frac{1}{\Gamma_p} \\ & - \int_{E_p}^{\infty} \frac{h}{E - E_p - i\Gamma_p} \text{Im} \frac{h}{\Gamma_p} \frac{1}{\Gamma_p} : \quad (51) \end{aligned}$$

Using the relation between the T-matrix element and the propagator of a localized d-level in the Anderson model,⁴⁵ $G_d(E_n; T)$, we find

$$h \Gamma_p = \Gamma_p(0) \Gamma_p(0) \Gamma_p^2 G_d : \quad (52)$$

Inserting this relation into Eq. (51), we find that the spin scattering rate is given by

$$\begin{aligned} \gamma_s(E; T) = & n_m \frac{\langle E; 0 \rangle}{\Gamma_0^2} \Gamma_0^2 \text{Im} G_d + \frac{\Gamma_0^4}{\Gamma_0^2} G_d^2 \\ = & \frac{\langle E; 0 \rangle}{\Gamma_0^2} \gamma_s^{(0)}(E; T) : \quad (53) \end{aligned}$$

where $\gamma_s^{(0)}$ is the inelastic spin scattering rate in a clean system which is a universal function of $T = T_K$ as has been shown in Refs. 45 and 46. Assuming that this equation still holds for a disordered metal, we may conclude that the spin scattering rate in the state E_n not only depends on the ratio $T = T_K$ but also explicitly depends on the local density of states. But both T_K and $\langle E; 0 \rangle$ are randomly distributed, taking different values for each magnetic impurity, and so will $\gamma_s(E; T)$. Note that

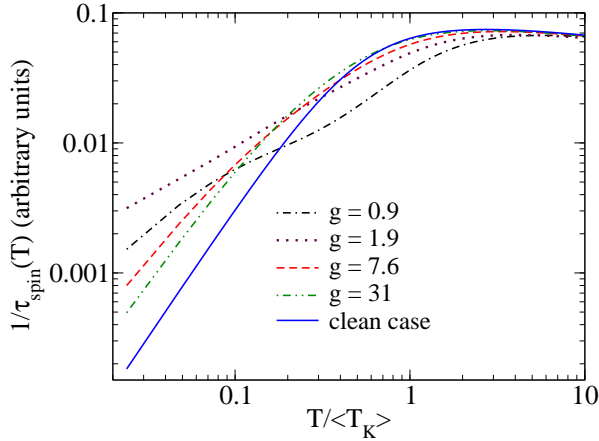


FIG. 12: The spin relaxation rate as a function of temperature for $J=D=0.24$. The broken lines correspond to ensemble averages of Eq. (53) over fluctuating Kondo temperatures and the LDOS at the Fermi energy. The solid line is obtained from Eq. (54) setting $T_K = \hbar T_K \approx 1$ (clean case).

the distribution of Kondo temperatures alone is not sufficient for determining the average spin scattering rate. We have seen in Sec. VI that in a two-dimensional metal the wave functions correlations at different energies are of order $1=g$. The probability of having simultaneously a small Kondo temperature and a small local density of states at the Fermi energy leading to an anomalous value for the spin scattering rate is expected to be of order $1=g$ as well.

We can derive the temperature dependence of the spin scattering rate in a sample with a finite number of magnetic impurities by averaging the dephasing rate of a single magnetic impurity over an ensemble of magnetic impurities. To facilitate the calculations, we approximate the universal function for the dephasing rate by the following function,

$$\frac{1}{\tau_s^{(0)}} = \frac{n_m S (S+1)}{\ln^2 \frac{T}{T_K}} + \frac{T_K^2}{T^2} + \frac{1}{T} \quad ; \quad (54)$$

with $= 0.2$, as found numerically in Ref. 45. Note that temperature scales with T_K only. Equation (54) coincides with Eq. (44) in both low- and high-temperature limits. In Fig. 12 we show the result of using Eq. (54) in Eq. (53) and ensemble averaging the spin relaxation rate over T_K and $(E_F; 0)$ obtained numerically for the disordered tight-binding model (see Sec. VI). One finds a clear departure from the clean case prediction at low temperatures,⁴⁶ which amounts to an enhancement of the spin scattering due to the presence of nonmagnetic disorder. A very similar behavior has been recently observed in weak-localization measurements performed by the Grenoble group on quasi-one-dimensional Ag wires doped with 2 to 20 ppm Fe impurities,⁵⁷ as well as by the Michigan group,⁵⁸ where similar samples where implanted with 2 to 10 ppm of Fe impurities. One should note that these samples have very high diffusion constants, of order $D_e = 300 - 400 \text{ cm}^2/\text{s}$,

so that the parameter g in these samples is large, $g > 100$. For the Fermi energy in Ag, $E_F = 5.5 \text{ eV}$, and the Kondo temperature of $T_K = 4 \text{ K}$, the ratio between band width and exchange coupling is found to be of the order of $J=D = 0.1$. Thus, according to Eq. (40), $T_K = \hbar T_K \approx 1$ is fulfilled and the width of the distribution of Kondo temperatures should be negligible in 2D samples. However, one has to be careful when considering the relevance of our results to the weak-localization experiments of Refs. 57 and 58. For instance, we note that the low-temperature dephasing rate is dominated by the non-Gaussian low- T_K tail of the distribution of the Kondo-temperature, which we have found to be present even for weak disorder, $g = 10$. Moreover, the samples used in Refs. 57 and 58 were quasi-one-dimensional, in which case T_K is known to be further enhanced.⁴⁶

In order to connect theory with experiments, some more work needs to be done. On the theoretical side, a systematic study of how the distribution of the Kondo temperature scales with the width and length of the sample is necessary. This is the subject of ongoing work and will be published elsewhere.⁵⁹ On the experimental side, the relevance of the distribution of the Kondo temperature to the low-temperature anomaly of the dephasing rate could be established by utilizing samples with lower diffusion constants, such as the low-mobility samples of AuPd, examined in Ref. 60. These have diffusion constants as low as $D_e = 13.4 \text{ cm}^2/\text{s}$, corresponding to $g = 17$. The presence of free magnetic moments would be facilitated in semiconductors such as Si and GaAs where the effective mass of electrons is smaller than in metals by a factor 30. Moreover, 2D electron gases with $a k_F \approx 1$ can be produced with those materials. In low-mobility GaAs wires, Anderson localization has been observed even in wires with $g = 30$.⁶¹ Thus, all mesoscopic energy scales can become relevant when the system reaches temperatures of the order of 1 K. However, so far no magnetic impurities with detectable Kondo temperatures have been found in semiconductors, since the low density of states suppresses the Kondo temperature exponentially.

IX. CONCLUSIONS

The screening of magnetic moments in metals, the Kondo effect, is found to be quenched with a finite probability in the presence of nonmagnetic disorder. For weak disorder, $g \approx 1$, the effect is shown analytically and numerically to be due to wave function correlations. Thus, the distribution of the Kondo temperature $P(T_K)$ retains a finite width in the limit of vanishing level spacing. When time-reversal symmetry is broken either by applying a magnetic field or by increasing the concentration of magnetic impurities, $P(T_K)$ becomes narrower. The probability that a magnetic moment remains free down to the lowest temperatures is found to increase with disorder strength. Magnetic impurities with a small Kondo temperature are shown to modify the temperature dependence of the dephasing rate at low temperatures, $T \ll \hbar T_K \approx 1$, as measured in weak-localization transport experiments.

Acknowledgments

The authors gratefully acknowledge useful discussions with Harold Baranger, Carlo Beenakker, Claudio Chamon, Peter Fulde, Ribhu Kaul, Vladimir Kravtsov, Caio Lewenkopf, Ganpathy Murthy, Mikhail Raikh, A. Rosch, Denis Ullmo, Isa Zarekeshev, and Andrey Zhuravlev. The authors thank the hospitality of the Condensed Matter Theory Group at Boston University, where this work was initiated, and the Aspen Center for Physics, where the manuscript was finalized. S.K. also acknowledges the hospitality of the Max-Planck Institute for Physics of Complex Systems and the Department of Physics at the University of Central Florida. E.R.M. thanks the hospitality of the Institute for Theoretical Physics at the University of Hamburg. This research was supported by the German Research Council (DFG) under SFB 508, A9, and SFB 668, B2.

APPENDIX A: DERIVATION OF EQ. (1)

We begin with the Anderson model, namely, a localized d-level coupled to a conduction band,¹⁸

$$H = \sum_{n=1}^N E_n \hat{n}_n + \sum_{d=1}^D E_d \hat{n}_d + U \hat{n}_{d+} \hat{n}_d + \sum_{n=1}^N t_{nd} c_n^+ c_d + t_{dn} c_d^+ c_n; \quad (A1)$$

where E_n are the eigenenergies of the conduction band electrons, E_d is the energy of a singly occupied d-level, and $E_d + U$ is the energy of a doubly occupied d-level. $t_{dn} = t_{nd}$ are the hybridization matrix elements between the d-level and the conduction band state $|n\rangle$. Projecting out of the Hilbert space all state where the d-levels are doubly occupied one obtains the Kondo Hamiltonian

$$H_J = J S \cdot S; \quad (A2)$$

where the matrix elements of the exchange interaction in the basis of the eigenstates of the conduction electrons are given by

$$J_{kl} = \frac{8 t_{kd} t_{dl}}{U}; \quad (A3)$$

These matrix elements are positive and thus the interaction is antiferromagnetic. The hopping matrix element connecting the localized d-state $|d\rangle$ to the conduction band state $|n\rangle$ is given by

$$t_{dn} = \int_{-\infty}^{\infty} d^d r \langle d(r) \hat{T}^n | n(r) \rangle; \quad (A4)$$

where \hat{T} is the kinetic energy operator. For a impurity state strongly localized at $r = 0$ we obtain

$$J_{kl} = J_d(0) \delta_{n,l}(0); \quad (A5)$$

where $J = 8(1-m/a_0^2)^2 U$, m is the band mass, and a_0 is the radius of the localized state at the magnetic atom. We define T_K by the divergence of second-order perturbation theory. To second order in J , there are two processes to be considered: (i) The scattering due to the exchange coupling J of an electron from state $|n\rangle$ to a state $|i\rangle$ close to the Fermi energy via an intermediate state $|m\rangle$. This process is proportional to the probability that state $|m\rangle$ is not occupied, $1 - f(E_m)$, where $f(E)$ is the Fermi distribution. (ii) The reverse process, in which a hole is scattered from the state $|i\rangle$ to the state $|n\rangle$ via the occupied of a state $|m\rangle$ with probability proportional to the occupation factor $f(E_m)$. Thus, we find that the exchange coupling is renormalized to

$$J_{nl} = J_{nl} \left(1 + \frac{J}{2N} \sum_m \frac{|j_m(0)|^2}{E_m - E_F} \tanh \frac{E_m - E_F}{2T} \right); \quad (A6)$$

For positive exchange coupling, $J > 0$, perturbation theory diverges as the temperature is lowered. Defining the Kondo temperature as the temperature where the second-order correction to the exchange coupling becomes equal to the bare coupling, we arrive at Eq. (1).

An equivalent expression can be derived from the renormalization group equation, which in the two-loop approximation is given by³¹

$$\begin{aligned} \frac{dJ}{dt} = J^2 \frac{(E_F +) + (E_F -)}{2D} \\ \frac{1}{2} \frac{J^3}{D^2} \frac{(E_F +)}{Z} \Big|_0^Z \frac{dE}{(1 + E =)^2} \\ \frac{1}{2} \frac{J^3}{D^2} \frac{(E_F -)}{Z} \Big|_0^Z \frac{dE}{(1 + E =)^2}; \end{aligned} \quad (A7)$$

where $t = \ln D = (2)$. Defining T_K as the value of t at which J flows to the band width D and solving Eq. (A7) for T_K , we obtain for a clean system

$$T_K^{(0)} = \frac{e}{2^{3/2}} \frac{J}{D} \exp(-D = J); \quad (A8)$$

However, if we keep only the first term on the right-hand side of Eq. (A7) - the one-loop term, we obtain a self-consistency equation for the Kondo temperature that reads

$$\ln \frac{T_K}{T_K^{(0)}} = \frac{1}{2} \int_{2T_K = D}^Z \frac{dt}{t} \frac{(E_F + D t=2)}{t}; \quad (A9)$$

For $T_K = 0$, Eq. (A9) coincides with the self-consistency equation obtained using perturbation theory, namely, Eq. (1).

¹ A. C. Hewson, *The Kondo Problem to Heavy Fermions* (Cambridge University Press, 1997).

² A. A. Abrikosov, *Fundamentals of the Theory of Metals* (North Holland, Amsterdam, 1988).

³ P. Nozières, *J. Low-Temp. Phys.* **17**, 3 (1974).

⁴ K. G. Wilson, *Rev. Mod. Phys.* **47**, 773 (1975).

⁵ R. N. Bhatt and D. S. Fisher, *Phys. Rev. Lett.* **68**, 3072 (1992).

⁶ A. Langenfeld and P. Wölfle, *Ann. Physik* **4**, 43 (1995).

⁷ R. K. Kaul, D. Ullmo, and H. U. Baranger, *Phys. Rev. B* **68**, R161305 (2003).

⁸ E. Miranda, V. Dobrosavljević, and G. Kotliar, *J. Phys. Cond. Mat.* **8**, 9871 (1996).

⁹ S. Kettemann and E. R. Mucciolo, *Pis'ma v ZhETF* **83**, 284 (2006) [*JETP Letters* **83**, 240 (2006)].

¹⁰ B. L. Altshuler and B. I. Shklovskii, *Zh. Eksp. Theor. Fiz.* **91**, 220 (1986) [*Sov. Phys. JETP* **64**, 127 (1986)].

¹¹ A. G. Aronov, V. E. Kravtsov, and I. V. Lerner, *Phys. Rev. Lett.* **74**, 1174 (1995).

¹² A. Altland and D. Fuchs, *Phys. Rev. Lett.* **74**, 4269 (1995).

¹³ S. Kettemann, *Phys. Rev. B* **59**, 4799 (1999).

¹⁴ W. B. Thimm, J. Kroha, and J. von Delft, *Phys. Rev. Lett.* **82**, 2143 (1999).

¹⁵ S. Suga and T. Ohashi, *J. Phys. Soc. Jpn.* **72** Suppl. A, 139 (2003).

¹⁶ Y. Nagaoka, *Phys. Rev.* **138**, 1112 (1965).

¹⁷ P. Fulde, *Electron Correlations in Molecules and Solids*, 2nd ed. (Springer, Berlin, 1993).

¹⁸ P. W. Anderson, *Phys. Rev.* **124**, 41 (1961); P. W. Anderson, G. Yuval, and D. R. Hamann, *Phys. Rev. B* **1**, 4464 (1970).

¹⁹ K. B. Efetov, *Supersymmetry in Disorder and Chaos* (Cambridge University Press, Cambridge, 1997).

²⁰ V. N. Prigodin and K. B. Efetov, *Phys. Rev. Lett.* **70**, 2932 (1993).

²¹ C. W. J. Beenakker, *Phys. Rev. B* **50**, 15170 (1994).

²² M. L. Mehta, *Random Matrices* (Academic Press, Boston, 1991).

²³ A. D. Mirlin, *Phys. Rep.* **326**, 259 (2000).

²⁴ M. Miller, D. Ullmo, and H. U. Baranger, *Phys. Rev. B* **72**, 045305 (2005).

²⁵ We did not use the eigenfunctions resulting directly from the diagonalization of the GOE and GUE matrices to compute the Kondo temperature for the following reason. Even though these eigenfunctions do obey the Porter-Thomas distributions individually, they are constrained by the normalization condition $\sum_{n=1}^N x_n = N$. That alone makes $T_K \rightarrow 0$ as J approaches D and T_K itself becomes of order D . While this is correct for a single-band lattice model, it is not adequate for describing a multi-band continuous system.

²⁶ R. K. Kaul, D. Ullmo, S. Chandrasekharan, and H. U. Baranger, *Europhys. Lett.* **71**, 973, (2005).

²⁷ S. Kettemann, in *Quantum Information and Decoherence in Nanosystems*, eds. D. C. Glattli, M. Sanquer, and J. Tran Thanh Van (The Gioi Publishers, 2004), p.259.

²⁸ I. S. Gradshteyn and I. M. Ryzhik, *Table of Integrals, Series, and Products* (Academic Press, San Diego, 1992).

²⁹ P. W. Anderson, *J. Phys. Chem. Solids* **11**, 26 (1959); A. A. Abrikosov and L. P. Gorkov, *Sov. Phys. JETP* **8**, 1090 (1958).

³⁰ Notice that in our model simulations the Kondo temperature is determined by summing over contributions from all eigenstates in the band. Therefore, a normalization constraint to the wave function intensities is embedded into T_K obtained from the disordered tight-binding model, but it is absent in the RMT simulations.²⁵ This constraint strongly affects the fluctuations of T_K at large val-

ues of J , when all states in the band contribute to the sum in Eq. (2). The most visible consequence is the hump seen at $J=D$ ¹.

³¹ G. Zaránd and L. Udvárdi, *Phys. Rev. B* **54**, 7606 (1996).

³² S. Chakravarty and C. Nayak, *Int. J. Mod. Phys. B* **14**, 1421 (2000).

³³ P. S. Cornaglia, D. R. Grempel, and C. A. Balseiro, *Phys. Rev. Lett.* **96**, 117209 (2006).

³⁴ S. Hikami, A. I. Larkin, and Y. Nagaoka, *Prog. Theor. Phys.* **63**, 707 (1980).

³⁵ A. A. Bobkov, V. I. Fal'ko, and D. E. Khmel'nitskii, *Sov. Phys. JETP* **71**, 393 (1990) [*Zh. Eksp. Teor. Fiz.* **98**, 703 (1990)].

³⁶ S. Kettemann and M. E. Raikh, *Phys. Rev. Lett.* **90**, 146601 (2003).

³⁷ C. H. Lewenkopf and H. A. Weidenmüller, *Phys. Rev. B* **71**, 121309 (2005).

³⁸ G. Bergmann, *Phys. Rev. Lett.* **58**, 1236 (1987); R. P. Peters *et al.*, *ibid.* **58**, 1964 (1987); C. Van Haesendonck, *et al.*, *ibid.* **58**, 1968 (1987).

³⁹ P. Mohanty and R. A. Webb, *Phys. Rev. Lett.* **84**, 4481 (2000).

⁴⁰ M. B. Maple, in *Magnetism*, edited by H. Suhl (Academic, New York, 1973), Vol. 5, p. 289.

⁴¹ I. Affleck and A. W. W. Ludwig, *Phys. Rev. B* **48**, 7297 (1993).

⁴² E. Müller-Hartmann and J. Zittartz, *Phys. Rev. Lett.* **26**, 428 (1971).

⁴³ H. Suhl, *Phys. Rev. A* **138**, 515 (1965).

⁴⁴ F. Schopfer, C. Bäuerle, W. Rabaud, and L. Saminadayar, *Phys. Rev. Lett.* **90**, 056801 (2003).

⁴⁵ G. Zaránd, L. Borda, J. von Delft, and N. Andrei, *Phys. Rev. Lett.* **93**, 107204 (2004).

⁴⁶ T. Micklitz, A. Altland, T. A. Costi, and A. Rosch, *Phys. Rev. Lett.* **96**, 226601 (2006).

⁴⁷ S. Adam, P. W. Brouwer, J. P. Sethna, and X. Waintal, *Phys. Rev. B* **66**, 165310 (2002); S. Braig, S. Adam, and P. W. Brouwer, *Phys. Rev. B* **68**, 035323 (2003).

⁴⁸ V. E. Kravtsov, private communication (2006).

⁴⁹ M. A. Ruderman and C. Kittel, *Phys. Rev.* **96**, 99 (1954); T. Kasuya, *Prog. Theor. Phys.* **16**, 45 (1956); K. Yosida, *Phys. Rev.* **106**, 893 (1957).

⁵⁰ W. Wei, G. Bergmann, and R. Peters, *Phys. Rev. B* **16**, 11751 (1988).

⁵¹ P. G. de Gennes, *J. Phys. Radium* **23**, 630 (1962).

⁵² I. V. Lerner, *Phys. Rev. B* **48**, 9462 (1993).

⁵³ A. Yu. Zyuzin and B. Z. Spivak, *Pis'ma Zh. Eksp. Teor. Fiz.* **43**, 185 (1986) [*JETP Lett.* **43**, 234 (1986)].

⁵⁴ G. Frossati, J. L. Tholence, D. Thoustrup, and R. Tournier, *Physica B* **84**, 33 (1976).

⁵⁵ A. H. Castro Neto and B. A. Jones, *Phys. Rev. B* **62**, 14975 (2000).

⁵⁶ Note that the spin scattering rate in Eq. (51) is 1/2 of the dephasing rate as defined in Ref. 46).

⁵⁷ F. Mallet, J. Ericsson, D. Mailly, S. Unlubayir, D. Reuter, A. Melnikov, A.D. Wieck, T. Micklitz, A. Rosch, T. A. Costi, L. Saminadayar, and C. Bauerle, preprint (cond-mat/0607154).

⁵⁸ G. M. Alzoubi and N. O. Birge, preprint (cond-mat/0607168).

⁵⁹ A. Zhuravlev, I. Zharekeshev, E. R. Mucciolo, and S. Kettemann, unpublished (2006).

⁶⁰ A. Trionfi, S. Lee, and D. Natelson, *Phys. Rev. B* **70**, R041304 (2004).

⁶¹ M. E. Gershenson, Yu. B. Khavin, A. G. Mikhalchuk, H. M. Bzozler, and A. L. Bogdanov, *Phys. Rev. Lett.* **79**, 725 (1997).